Pheromone-induced anisotropy in yeast plasma membrane phosphatidylinositol-4,5-*bis*phosphate distribution is required for MAPK signaling

Lindsay S. Garrenton[a,1,2], Christopher J. Stefan[b,1], Michael A. McMurray[a], Scott D. Emr[b], and Jeremy Thorner[a,3]

[a]Division of Biochemistry and Molecular Biology, Department of Molecular and Cell Biology, University of California, Berkeley, CA 94720-3202; and [b]Weill Institute for Cell and Molecular Biology, Cornell University, Ithaca, NY 14853-7202

Communicated by Alexander Namiot Glazer, University of California, Berkeley, CA, May 4, 2010 (received for review February 22, 2010)

During response of budding yeast to peptide mating pheromone, the cell becomes markedly polarized and MAPK scaffold protein Ste5 localizes to the resulting projection (shmoo tip). We demonstrated before that this recruitment is essential for sustained MAPK signaling and requires interaction of a pleckstrin homology (PH) domain in Ste5 with phosphatidylinositol 4,5-*bis*phosphate [PtdIns(4,5)P_2] in the plasma membrane. Using fluorescently tagged high-affinity probes specific for PtdIns(4,5)P_2, we have now found that this phosphoinositide is highly concentrated at the shmoo tip in cells responding to pheromone. Maintenance of this strikingly anisotropic distribution of PtdIns(4,5)P_2, stable tethering of Ste5 at the shmoo tip, downstream MAPK activation, and expression of a mating pathway-specific reporter gene all require continuous function of the plasma membrane-associated PtdIns 4-kinase Stt4 and the plasma membrane-associated PtdIns4P 5-kinase Mss4 (but not the Golgi-associated PtdIns 4-kinase Pik1). Our observations demonstrate that PtdIns(4,5)P_2 is the primary determinant for restricting localization of Ste5 within the plasma membrane and provide direct evidence that an extracellular stimulus-evoked self-reinforcing mechanism generates a spatially enriched pool of PtdIns(4,5)P_2 necessary for the membrane anchoring and function of a signaling complex.

α-factor | phosphoinositides | scaffold protein | yeast mating response

Eukaryotic cells respond to extracellular stimuli and spatial cues via signaling responses that can dramatically alter cell polarity. Ample evidence from diverse cell types indicates that membrane phosphoinositides, especially phosphatidylinositol 4,5-*bis*phosphate [PtdIns(4,5)P_2] (1), are key regulators of processes, like cytoskeletal remodeling (2) and vesicle-mediated trafficking (3, 4), which are required for polarized growth, cell morphogenesis, and cell division (5). In both mammalian leukocytes and migratory *Dictyostelium discoideum* amoebae, exposure to chemoattractant results in spatial restriction of PtdIns(3,4,5)P_3, as well as of the enzymes that catalyze its synthesis (PtdIns 3-kinase) and breakdown [phosphatidylinositol 3-phosphatase and tensin homolog (PTEN)] (6). Likewise, in mammalian kidney cells, localized action of the PtdIns(3,4,5)P_3 phosphatase PTEN plays a key role in determining epithelial cell polarity by defining the content of this lipid in the apical and basolateral membranes (7), thereby affecting the distribution of small GTPases that dictate cell shape (8). Membrane phosphoinositides were also shown to play an important role in driving anchor cell invasion during *Caenorhabditis elegans* development (9). These examples all indicate that membrane subdomains enriched for specific phosphoinositides are crucial for attracting signaling components specific for establishment and/or maintenance of cell polarity.

Likewise, in *Saccharomyces cerevisiae*, phosphoinositides in the plasma membrane have been implicated in the recruitment of proteins involved in polarized morphogenesis, cytoskeletal rearrangement, and endocytic trafficking during vegetative growth (10). However, no role had been ascribed to PtdIns(4,5)P_2 in the response of yeast cells to any extracellular signal until we demonstrated that pheromone-stimulated recruitment of the MAPK scaffold Ste5 to the shmoo tip is dependent on the PtdIns(4,5)P_2-binding ability of a pleckstrin homology (PH) domain in Ste5 (11). These observations raised the possibility that PtdIns(4,5)P_2 itself is enriched at the shmoo tip, providing a spatial landmark to facilitate establishment of the observed highly polarized distribution of Ste5.

Here we show, using two high-affinity probes for PtdIns(4,5)P_2, that there is a highly anisotropic distribution of PtdIns(4,5)P_2 at the shmoo tip in cells responding to pheromone. Inactivation of plasma membrane-associated lipid kinases Stt4 and Mss4 abolished PtdIns(4,5)P_2 anisotropy, prevented localization of the Ste5 at the shmoo tip, and markedly decreased activation of the mating response. These findings are direct evidence that a spatially enriched pool of PtdIns(4,5)P_2 has an essential role in tethering a signaling complex to the membrane in response to an extracellular stimulus and in maintaining the function of that complex for signal propagation.

Results and Discussion

Pheromone Action Generates a Highly Polarized PtdIns(4,5)P_2 Distribution. To monitor dynamic changes in the pattern of PtdIns(4,5)P_2 distribution in the plasma membrane, we used two different fluorescent probes, GST-GFP-PH$^{PLC\delta1}$ and GFP-2XPH$^{PLC\delta1}$, each marked with eGFP and containing the PH domain of mammalian PLCδ1, which has been shown to bind to PtdIns(4,5)P_2 with high specificity (12) and high affinity ($K_d \leq 2$ μm) (13). To increase avidity and selectivity, each probe contains dual PLCδ1 PH domains, either paired by GST-mediated dimerization (14) or encoded in tandem (15). Using either probe, we found that, in vegetative cells, PtdIns(4,5)P_2 is reproducibly enriched in areas of polarized growth, in particular, the incipient bud site, the bud, and at the bud neck, especially during cytokinesis (Fig. 1*A Left* and Fig. S1). However, the most striking enrichment was seen at the shmoo tip in pheromone-treated cells, whether observed by standard epifluorescence microscopy (Fig. 1*A Right*) or by deconvolution microscopy (Fig. 1*B*). Marked concentration of PtdIns(4,5)P_2 at the shmoo tip could be observed as soon as a mating projection was discernible (within 15–20 min) and was further strengthened and maintained throughout the time course of our observations (for at least 90 min) (Fig. 1*A*). The observed gradient is not due to preferential degradation of the probe away from the shmoo tip in

Author contributions: L.S.G., C.J.S., S.D.E., and J.T. designed research; L.S.G., C.J.S., and M.A.M. performed research; L.S.G., C.J.S., S.D.E., and J.T. analyzed data; and L.S.G. and J.T. wrote the paper.

The authors declare no conflict of interest.

Freely available online through the PNAS open access option.

[1]L.S.G. and C.J.S. contributed equally to this work.

[2]Present address: Department of Cell Regulation, Genentech Inc., 1 DNA Way, South San Francisco, CA 94080.

[3]To whom correspondence should be addressed. E-mail: jthorner@berkeley.edu.

This article contains supporting information online at www.pnas.org/lookup/suppl/doi:10.1073/pnas.1005817107/-/DCSupplemental.

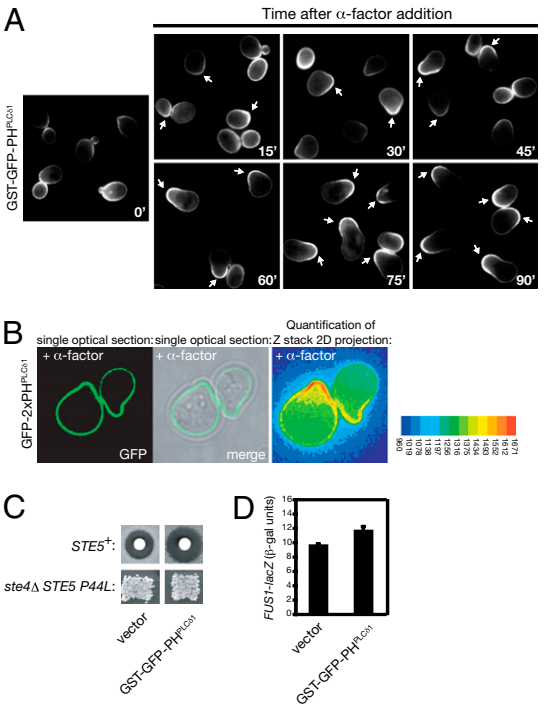

Fig. 1. Fluorescent reporters reveal highly polarized PtdIns(4,5)P_2 distribution during pheromone response and do not perturb signaling. (*A*) Exponentially-growing wild-type cells (strain BY4741) carrying a 2-μm DNA vector expressing from the *GAL1* promoter the PtdIns(4,5)P_2-binding GST-GFP-$PH^{PLC\delta1}$ probe were induced by addition of galactose for 30 min and then harvested by brief centrifugation, washed, and resuspended in glucose-containing medium to shut off any further probe expression. After 15 min, the cells were treated with 5 μM α-factor, and samples were withdrawn every 15 min, as indicated, and examined by standard epifluorescence microscopy. Each panel depicts a collage of representative cells at each time point; arrows denote the tips of mating projections that exhibited marked asymmetric distribution of the probe. (*B*) Strain YCS234 carrying a 2-μm DNA vector (pRS426) expressing from the constitutive *PRC1* promoter an alternative PtdIns(4,5)P_2-binding probe (GFP-2XP$H^{PLC\delta1}$) was treated with 0.1 μM α-factor for 1 h, spread on an agar pad, and examined by deconvolution microscopy. False color image represents the indicated scale of measured pixel intensity. (*C*) *Upper*, strain BY4741 was transformed with an empty 2-μm DNA vector or the same plasmid expressing GST-GFP-$PH^{PLC\delta1}$ from the *GAL1* promoter (pPP1872), as indicated and tested for sensitivity to pheromone-induced growth arrest by halo bioassay on galactose-containing medium. *Lower*, strain BYB88 (*ste4Δ ste5Δ*) was cotransformed with a *URA3*-marked 2-μm DNA vector expressing from the *GAL1* promoter the hyperactive Ste5(P44L) allele and a *LEU2*-marked *CEN* vector expressing GST-GFP-$PH^{PLC\delta1}$ from the *GAL1* promoter (pLG99) and tested for mating proficiency by patch mating assay on galactose-containing medium. (*D*) Strain YLG36 carrying a $FUS1_{prom}$-*lacZ* reporter gene was transformed with an empty 2-μm DNA vector or the same plasmid expressing GST-GFP-$PH^{PLC\delta1}$, as indicated. Representative transformants (n = 3) of each type were grown to early exponential phase, induced with galactose for 2 h, and treated with 3 μM α-factor for 90 min, and expression of β-galactosidase was measured (mean ± SD).

response to pheromone because both probes remained stable in the absence or the presence of pheromone (Fig. S2). Likewise, the observed gradient could not be attributed to preferential immobilization of the probe at the shmoo tip because analysis of probe dynamics by fluorescence recovery after photobleaching (FRAP) indicated that its mobility at that location is, if anything, slightly greater than elsewhere on the plasma membrane (Movie S1 and Fig. S3). Although PtdIns(4,5)P_2 is enriched in specialized plasma membrane regions in mammalian cells, such as in phagosomes, membrane ruffles, lamellipodia, and the cleavage furrow (16), our findings are, to our knowledge, unique evidence for a spatially segregated pool of PtdIns(4,5)P_2 generated in response to an extracellular signal.

A potential drawback in using lipid-binding chimeras is the possibility that they mask endogenous phosphoinositides, or otherwise influence their levels or distribution, and thereby perturb cellular processes dependent on them. However, we ruled out this concern for the GST-GFP-$PH^{PLC\delta1}$ probe because even continuous high-level (*GAL1* promoter-driven) expression did not inhibit pheromone response as assessed either by the standard halo bioassay for pheromone-induced G1 arrest (Fig. 1*C Upper*) or by induction of a mating pathway-specific reporter gene ($FUS1_{prom}$-*lacZ*) (Fig. 1*D*). Likewise, the GFP-2XP$H^{PLC\delta1}$ probe had no effect in either assay. Also, we examined whether probe expression affected mating proficiency in a sensitized assay. For this purpose, we used Ste5(P44L), a mutant that bypasses its requirement for Gβγ-dependent membrane anchoring and relies on its other two membrane-targeting elements for signal propagation, an N-terminal amphipathetic helix (PM motif) (17) and its PH domain (11). In the absence of PtdIns(4,5)P_2 binding by the PH domain, Ste5(P44L) is unable to support mating (11). Continuous high-level expression of GST-GFP-$PH^{PLC\delta1}$ had no detectable effect on the ability of Ste5(P44L) to support mating (Fig. 1*C Lower*). Because three independent readouts of pheromone response were not inhibited, the probes likely report the physiological relevant distribution of PtdIns(4,5)P_2.

Continuous Lipid Kinase Function Is Required for Maintenance of PtdIns(4,5)P_2 Anisotropy. To determine whether the anisotropy in plasma membrane PtdIns(4,5)P_2 observed in response to pheromone reflects redistribution of preexisting molecules or requires new synthesis, and to identify proteins involved in establishing and maintaining this gradient, we examined partitioning of the GST-GFP-$PH^{PLC\delta1}$ probe in cells carrying temperature-sensitive (*ts*) mutations in the lipid kinases known to be required for PtdIns(4,5)P_2 production (10). In the control (otherwise isogenic wild-type cells), the probe was localized in the expected asymmetric fashion by 30 min after pheromone treatment and this pattern was maintained after shift to 37 °C for 1 h (Fig. 2*A*). In contrast, in cells carrying a *ts* allele in the PtdIns4P 5-kinase Mss4, the probe was enriched in the mating projection at the permissive temperature, but this localization was lost completely after the shift to restrictive temperature (Fig. 2*B*), even though shmoo morphology was maintained. Thus, active synthesis of PtdIns(4,5)P_2 [rather than sequestration of preexisting PtdIns(4,5)P_2 molecules] is required to generate the observed polarized distribution of this lipid.

To determine whether this pool of PtdIns(4,5)P_2 arises by local synthesis at the plasma membrane or is delivered to the plasma membrane via vesicle-mediated transport, we examined probe distribution in mutants carrying *ts* alleles in two essential PtdIns 4-kinases that produce the immediate precursor to PtdIns(4,5)P_2: Stt4, which generates PtdIns4P at the plasma membrane (18), and Pik1, which generates PtdIns4P in the Golgi compartment (19). In both mutants, the probe decorated the shmoo tip at the permissive temperature, as anticipated; however, after shift to the restrictive temperature, the probe failed to localize asymmetrically to the shmoo tip in the $stt4^{ts}$ cells (Fig. 2*C*), but was maintained normally in the $pik1^{ts}$ cells (Fig. 2*D*), indicating that the supply of PtdIns4P to make the PtdIns(4,5)P_2 found at the shmoo tip does not come via vesicle-mediated delivery, but rather by Stt4-mediated synthesis in situ. Consistent with this conclusion, in the majority of the $stt4^{ts}$ cells, there was not only no enrichment, but also a noticeable decrease, in the amount of probe present at the shmoo tip, as compared with the rest of the plasma membrane (Fig. 2*C*). As expected, in an $stt4^{ts}$ $pik1^{ts}$ double mutant, the $stt4^{ts}$ phenotype was epistatic (Fig. 2*E*). We did note, however, that, even at permissive temperature, there was a modest decrease in the number of cells that exhibited the signal-induced anisotropy in GST-GFP-$PH^{PLC\delta1}$ distribution in both the $pik1^{ts}$ single mutant

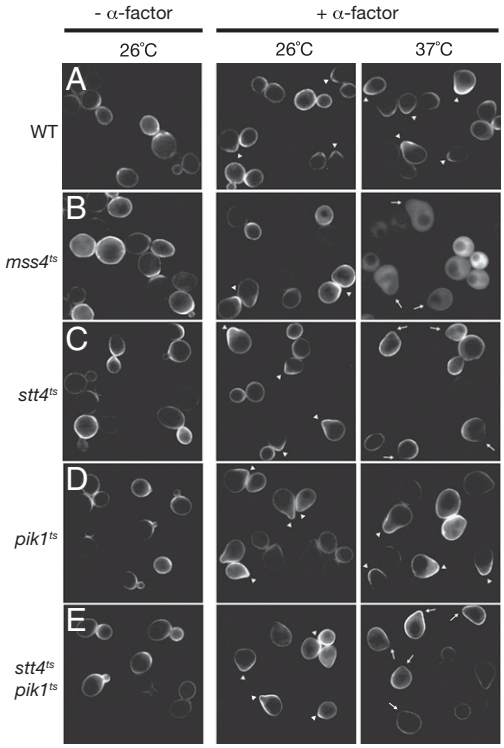

Fig. 2. Continuous synthesis is required for maintenance of PtdIns(4,5)P_2 anisotropy in the plasma membrane during pheromone response. (*A–E*) Expression of the GST-GFP-PH$^{PLC\delta1}$ probe was induced and shut off, as described in Fig. 1*A*, in either wild-type cells (*A*) or otherwise isogenic *mss4^{ts}* (*B*), *stt4^{ts}* (*C*), *pik1^{ts}* (*D*), or *stt4^{ts} pik1^{ts}* (*E*) mutants. After 15 min, each culture was treated with 5 μM α-factor for 30 min, at which point half of each culture was left at the permissive temperature (26 °C) and half was shifted to the restrictive temperature (37 °C). After 1 h, cells in each culture were examined by standard epifluorescence microscopy. Each panel depicts a collage of representative cells at each time point: *arrowheads*, mating projections with a marked asymmetric distribution of the PtdIns(4,5)P_2 probe; *arrows*, mating projections lacking a marked asymmetric distribution of the probe.

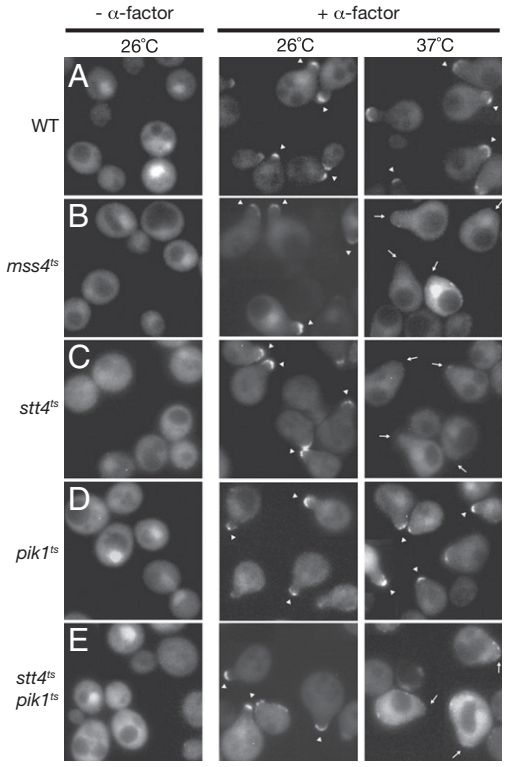

Fig. 3. Continuous PtdIns(4,5)P_2 synthesis is required for stable accumulation of Ste5 at the shmoo tip during pheromone response. (*A–E*) Exponentially growing cultures of *ste5Δ* cells (*A*), *ste5Δ mss4^{ts}* cells (*B*), *ste5Δ stt4^{ts}* cells (*C*), *ste5Δ pik1^{ts}* cells (*D*), or *ste5Δ stt4^{ts} pik1^{ts}* cells (*E*), each harboring a low-copy (*CEN*) vector expressing from the *STE5* promoter Ste5-$(GFP)_3$, were treated with 20 μM α-factor for 30 min, at which point half of each culture was left at the permissive temperature (26 °C) and half was shifted to the restrictive temperature (37 °C). After 90 min, cells in each culture were examined by standard epifluorescence microscopy. Each panel depicts a collage of representative cells at each time point: *arrowheads*, mating projections where Ste5-$(GFP)_3$ accumulated; *arrows*, mating projections lacking Ste5-$(GFP)_3$.

and the *stt4^{ts} pik1^{ts}* double mutant. Because Pik1 is required for the Golgi-to-plasma membrane step in vesicle-mediated secretory transport (19), this effect most likely reflects that polarized growth and, hence, initial shmoo formation occur somewhat less efficiently because Pik1 function is partially compromised in this *pik1^{ts}* mutant even under permissive conditions.

Stable Anchoring of Ste5 at the Projection Tip Requires the PtdIns(4,5)P_2 Gradient. Because localization of Ste5 to the shmoo tip requires the function of its PtdIns(4,5)P_2-binding PH domain (11), membrane binding of Ste5 should behave like the PtdIns(4,5)P_2-binding probe, if PtdIns(4,5)P_2 itself is indeed the primary determinant of Ste5 recruitment. Therefore, we examined in the same fashion the subcellular distribution of a fully functional Ste5-$(GFP)_3$ fusion (11, 17) expressed from its own promoter as the sole source of Ste5 in wild-type cells and in the isogenic *mss4^{ts}*, *stt4^{ts}*, and *pik1^{ts}* mutants. At the permissive temperature, Ste5-$(GFP)_3$ displayed the characteristic shmoo tip localization in all of the cell types examined (Fig. 3). However, and as observed for the PtdIns(4,5)P_2 probe itself, after shift to the restrictive temperature, shmoo tip localization of Ste5 was maintained in >90% of the wild-type cells (Fig. 3*A*) and the *pik1^{ts}* mutant (Fig. 3*D*), but abolished in >90% of the *mss4^{ts}* and *stt4^{ts}* single mutants and the *stt4^{ts} pik1^{ts}* double mutant (Fig. 3 *B*, *C*, and *E*). Thus, maintenance of plasma membrane anisotropy in PtdIns(4,5)P_2 distribution is required for the corresponding enrichment and stable tethering of Ste5 at the shmoo tip.

Stable Anchoring of Ste5 at the Projection Tip Does Not Require Actin Filaments or PtdIns 3-Kinase. As mentioned earlier, in many cell types, membrane phosphoinositides have been linked to actin filament dynamics and function via the action of small Rho and Rac family GTPases. Likewise, in the same way, PtdIns(4,5)P_2 plays an essential role in proper actin cytoskeleton organization during polarized growth in *S. cerevisiae* (20). Moreover, it has been reported that Ste5 is transported to the shmoo tip on actin cables (21). Therefore, it was conceivable that loss of Ste5 from the shmoo tip in the absence of continuous PtdIns(4,5)P_2 synthesis at the plasma membrane was simply an indirect effect of perturbing actin function. To rule out this possibility, we examined Ste5-$(GFP)_3$ localization in cells treated with the potent actin depolymerizing agent latrunculin-A (Lat A) (22) either before or after pheromone stimulation. In agreement with the requirement for actin function in polarized growth, treatment with Lat A before pheromone treatment blocked subsequent shmoo formation, but did not prevent membrane recruitment of Ste5, which appeared as puncta dispersed around the cell perimeter (Fig. 4*A Upper*). Moreover, once shmoos were formed and Ste5 accumulated at the shmoo tip, maintenance of Ste5 at this location was unaffected by Lat A treatment (Fig. 4*A Lower*). These results indicate that continuous actin-dependent delivery

is not necessary for Ste5 association with the membrane and not necessary to maintain Ste5 at the shmoo tip, consistent with our observation that the absence of vesicle-mediated transport in *pik1*^{ts} cells does not abrogate either the PtdIns(4,5)P_2 gradient (Fig. 2*D*) or Ste5 localization to the membrane (Fig. 3*D*). These findings also further solidify the conclusion that the Stt4- and Mss4-dependent anisotropy in PtdIns(4,5)P_2 distribution is indeed the crucial factor for localizing and tethering Ste5 at the tip of the mating projection.

In yeast, the Gα subunit (Gpa1) of the pheromone-receptor-coupled heterotrimeric G protein serves primarily a negative role in constraining the positively acting functions of the Gβγ complex (23). However, it has been reported (24) that, during pheromone response, Gpa1 localizes to endosomes where it activates PtdIns 3-kinase Vps34, which produces PtdIns3P, but its role in mating physiology is unclear. Although *vps34*Δ mutants have abnormal vacuoles and defects in protein trafficking to the vacuole and in autophagy (10), they are viable. Therefore, to address whether PtdIns(4,5)P_2 anisotropy during the mating response depends on PtdIns 3-kinase function in endosomal sorting or recycling pathways, we examined whether a complete null allele (*vps34*Δ) had

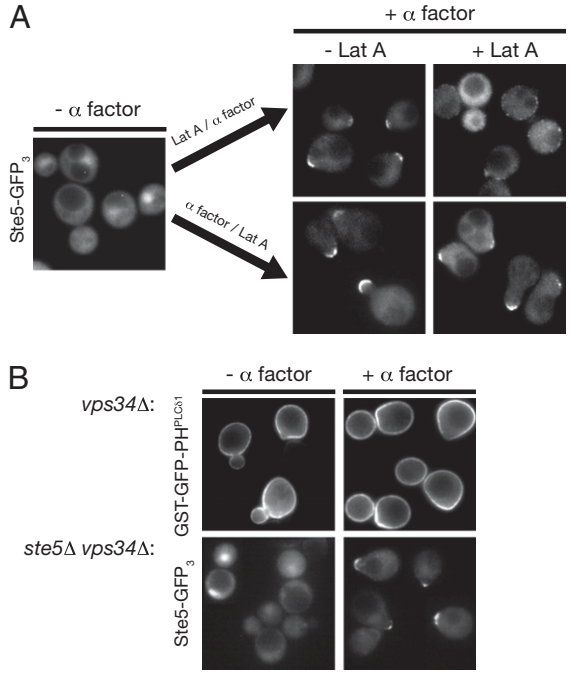

Fig. 4. Membrane recruitment and shmoo tip localization of Ste5 do not require actin filament function or PtdIns 3-kinase Vps34 activity. (*A*) Exponentially growing cultures of *ste5Δ* cells harboring a low-copy (*CEN*) vector expressing from the *STE5* promoter Ste5-$(GFP)_3$ (*Left*) were either not treated (–) or treated (+) with 100 μM latrunculin A (Lat A) for 15 min and then treated with 20 μM α-factor for 30 min (*Right, Upper*) or treated with 20 μM α-factor for 30 min and then either not treated (–) or treated (+) with 100 μM Lat A for 30 min (*Right, Lower*). Cells were then examined by standard epifluorescence microscopy; each panel depicts a collage of representative cells. (*B*) *Upper*, PtdIns 3-kinase Vps34 is not required to generate PtdIns(4,5)P_2 anisotropy. Expression of the GST-GFP-PH^{PLCδ1} probe was induced and shut off in a *vps34*Δ mutant as described in Fig. 1*A*, and the cells then were either not treated (–) or treated (+) with 5 μM α-factor for 60 min and examined by standard epifluorescence microscopy. *Lower*, PtdIns 3-kinase Vps34 is not required for plasma membrane recruitment of Ste5. Exponentially growing cultures of a *ste5Δ vps34Δ* double mutant harboring a low-copy (*CEN*) vector expressing from the *STE5* promoter Ste5-$(GFP)_3$ were either not treated (–) or treated (+) with 20 μM α-factor for 90 min and examined by epifluorescence microscopy. Each panel depicts a collage of representative cells.

any discernible effect on the pheromone-induced plasma membrane PtdIns(4,5)P_2 gradient, shmoo formation, or recruitment of Ste5 to the projection tip. Absence of Vps34 had no detectable effect on any of these processes (Fig. 4*B*). Moreover, in our hands, there was no diminution of MAPK activation (Fig. 5 *A* and *B*) or of transcriptional output (Fig. 5*C*) in response to pheromone in *vps34*Δ cells.

Maintnance of Robust MAPK Signaling Requires the PtdIns(4,5)P_2 Gradient. The data we have presented show that a highly anisotropic distribution of PtdIns(4,5)P_2 is required for stable retention of the Ste5 scaffold and, presumably, its associated MAPK components at the shmoo tip and thus should be a prerequisite for efficacious downstream signal propagation. Indeed, we demonstrated before that interaction of Ste5 via its PH domain with this phosphoinositide is essential for signaling (11). These considerations predicted that inactivation of the lipid kinases Stt4 and Mss4, which we showed are required to generate the plasma membrane PtdIns(4,5)P_2 gradient, should prevent pathway stimulation. Therefore, we examined two independent measures of pathway activation in response to pheromone in wild-type cells and in isogenic *mss4*^{ts}, *stt4*^{ts}, *pik1*^{ts}, *stt4*^{ts} *pik1*^{ts}, and *vps34*Δ mutants. First, using an antibody specific for phospho-MAPK (Fig. 5*A*), we found that all of the mutants converted an equivalent fraction of the total Fus3 to the activated state at the permissive temperature after α-factor addition (65–80% of that of the control cells) (Fig. 5*B*). At the nonpermissive temperature, Fus3 activation was reduced somewhat even in the control cells; however, Fus3 phosphorylation was reduced much more markedly in the *mss4*^{ts}, *stt4*^{ts}, and *stt4*^{ts} *pik1*^{ts} mutants (Fig. 5*A*, compare lanes 5, 7, and 11 to lane 3) than in the *pik1*^{ts} mutant (Fig. 5*B*). Moreover, as expected for elimination of only the Ste5-dependent route of MAPK activation, pheromone-induced phosphorylation of the related MAPK Kss1 (23) was less sensitive to inactivation of Mss4 and Stt4 than Fus3 phosphorylation (Fig. 5*A*). Taken together, our cytological and biochemical results are consistent with prior evidence (25, 26) and recent structural analysis indicating that Fus3 requires allosteric modulation by Ste5 for its activation by Ste7, whereas Kss1 does not (27). We also examined pathway activation in response to pheromone using a transcriptional reporter gene (Fig. 5*C*). In agreement with the other findings presented, loss of Mss4 and Stt4 dramatically reduced *FUS1*$_{prom}$-*lacZ* expression. Expression was also compromised in the *pik1*^{ts} mutant at restrictive temperature, but this possibility was anticipated (see *SI Text* for the explanation).

Collectively, this work shows that PtdIns(4,5)P_2 becomes enriched at the shmoo tip in response to pheromone and that the membrane localization and signaling function of Ste5 are completely dependent on this signal-evoked PtdIns(4,5)P_2 anisotropy. To begin to address the mechanism whereby this pheromone-induced PtdIns(4,5)P_2 gradient is generated, we envisioned several scenarios for how a Fus3-driven positive feedback loop might be involved, including a MAPK-regulated change in subcellular localization of the Stt4 and/or Mss4 kinases, MAPK-mediated local activation of the Stt4 and/or Mss4 kinases, or MAPK-imposed local inhibition of a plasma membrane PtdIns(4,5)P_2 5-phosphatase, such as Inp52/Sjl2 (15, 28). In contrast to the PtdIns(4,5)P_2 enrichment observed at the cleavage furrow in mammalian cells, where a PtdIns4P 5-kinase seems to be concentrated (29, 30), we found that Mss4 and Stt4 appear in discrete puncta rather uniformly distributed around the plasma membrane both before and during pheromone response (Fig. S4 *A* and *B*). Thus, it seems more likely that enhanced local activation of Sst4 and/or Mss4 or local inhibition of Sjl2 or other lipid phosphatases (or both) generates the pronounced pool of PtdIns(4,5)P_2 at the shmoo tip. Because the total cellular content of PtdIns(4,5)P_2 remains essentially constant upon pheromone treatment (Fig. S5),

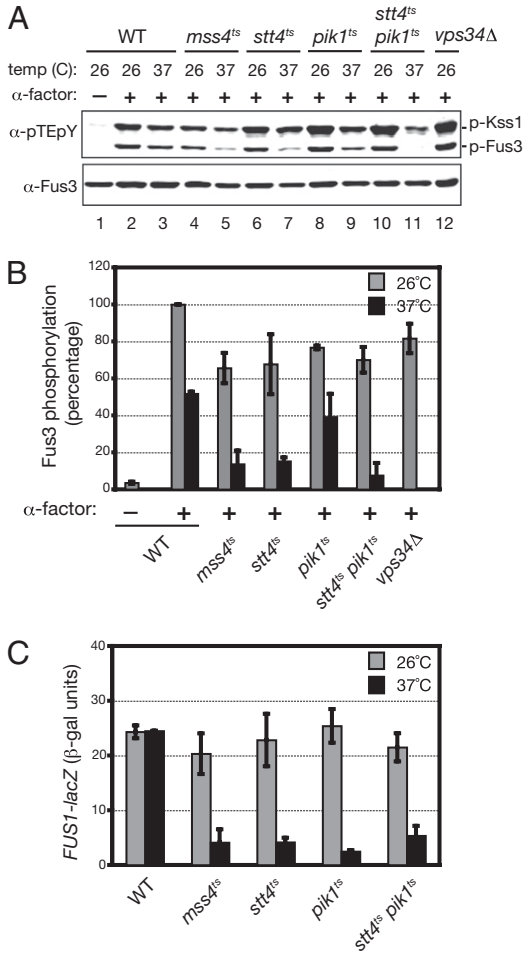

Fig. 5. Plasma membrane PtdIns(4,5)P_2 is necessary for MAPK activation and signaling. (*A*) Exponentially growing cultures of wild-type cells (strain YPH499) and otherwise isogenic *mss4^{ts}*, *stt4^{ts}*, *pik1^{ts}*, *stt4^{ts} pik1^{ts}*, and *vps34Δ* mutants, as indicated, were each divided into two equal portions, which were incubated for 45 min at either permissive (26 °C) or restrictive (37 °C) temperature, as indicated. Cells then were treated with 5 μM α-factor for 30 min, harvested, and ruptured by alkaline lysis and TCA precipitation (*Materials and Methods*). Samples of the resulting extracts were resolved by SDS/PAGE and immunoblotted with anti-phospho-p44/p42 and anti-Fus3 antisera. A representative experiment is shown. (*B*) Plots show the extent of Fus3 phosphorylation, relative to the level of total Fus3 in the same samples, normalized to the amount of Fus3 phosphorylated in the wild-type control cells at 26 °C (set at 100%). Values represent the average of three independent experiments (error bars represent the SE of those means). (*C*) Continuous phosphoinositide production at the plasma membrane and in the nucleus is required for pheromone-induced reporter gene expression. Independent cultures (n = 6) of wild-type cells or of the otherwise isogenic mutant strains indicated, each carrying a copy of the *FUS1$_{prom}$-lacZ* reporter gene integrated into their genome (strains YLG70, YLG71, YLG72, YLG73, and YLG74), were grown at 26 °C, divided into two portions, one of which was maintained at 26 °C (shaded bars) and the other of which was shifted to 37 °C for 45 min (solid bars), and then treated with 5 μM α-factor for 60 min. The cells in each culture were then harvested and the amount of β-galactosidase produced by each was measured (value given represents the mean and error bars represent ±SD).

we favor the view that the shmoo tip represents a privileged compartment where PtdIns(4,5)P_2 is generated at a normal rate, but protected from degradation by lipid phosphatases. Because Sjl2 function is partially redundant with that of both Inp51/Sjl1 and Inp53/Sjl3 (28), we examined probe distribution in double mutants treated with pheromone and indeed found that the combined actions of Sjl2 and Sjl3 are needed for establishment and/or maintenance of the plasma membrane PtdIns(4,5)P_2 gradient (Fig. S6). Moreover, modeling of lipid turnover and diffusion rates predicts that local synthesis alone may not be sufficient to maintain a PtdIns(4,5)P_2 gradient and that diffusion of this lipid needs to be restricted by other mechanisms (16). In this regard, double-labeling experiments suggest that the plasma membrane-associated septin meshwork may help confine the PtdIns(4,5)P_2 to the shmoo tip in cells responding to pheromone (Fig. S7) and perhaps demarcate a compartment that Sjl2 and/or Sjl3 cannot enter. In addition to Ste5, other components of the pheromone signaling machinery contain phosphoinositide-binding domains (e.g., Far1, Cdc24, and Bem1) (23). Therefore, the PtdIns(4,5)P_2 landmark described here may be a critical nexus for integrating optimally the complex signaling events required for pheromone response.

Materials and Methods

Yeast Strains and Media. Cultivation of yeast strains (Table S1) was at 30 °C (unless otherwise indicated) in standard rich (YP) or defined minimal (SC) media, containing 2% glucose (Glc), 2% raffinose with 0.2% sucrose (Raf-Suc), or 2% galactose (Gal) and supplemented with appropriate nutrients to maintain selection for plasmids, where necessary. For transient gene induction from the *GAL1* promoter, cells were pregrown to midexponential phase in the appropriate SC medium with Raf-Suc as the carbon source and then galactose was added to a final concentration of 2% to induce expression for the indicated lengths of time, after which cells were washed and resuspended in glucose-containing medium. To retard pheromone proteolysis during pheromone treatment, culture media were adjusted to a final concentration of 50 mM Na-succinate, pH 3.5, before addition of α-factor (31). To reduce autofluorescence in any strains bearing *ade* mutations, all media were supplemented with a final concentration of 20 mg/L of exogenous adenine. Standard techniques for propagation and genetic manipulation of yeast were used (32).

Plasmids and Recombinant DNA Methods. Plasmids were constructed and propagated in *Escherichia coli* using standard recombinant DNA methods (33). The PtdIns(4,5)P_2-specific fluorescent probes, pGST-GFP-PH$^{PLC\delta1}$ (pPP1872) (17) and pGFP-2xPH$^{PLC\delta1}$ (15) have been described previously. To generate pLG99, a *LEU2*-marked derivative of pPP1872, an XbaI-SalI fragment encoding pGST-GFP-PH$^{PLC\delta1}$ with the *GAL1* promoter sequence from pPP1872 was cloned into pRS315. The *CEN* plasmid pSTE5$_{prom}$-STE5-3xGFP (pPP1968) (17) used to visualize localization of Ste5 expressed at a near-endogenous level has been described previously. pCS7, expressing (His)$_6$-myc-Ste5(P44L) from the *GAL* promoter, was also described before (26).

Mating Response Assays. Mating proficiency of *MAT***a** cells was assessed qualitatively by the ability to produce a patch of diploid prototrophs using strain DC17 as the *MATα* tester (34). Briefly, patches of the *MAT***a** cells to be tested on an agar surface were replica plated onto a lawn of DC17 cells on YP medium containing as the carbon source either 2% glucose or 2% galactose [depending on the promoter controlling expression of the PtdIns(4,5)P_2-binding probe]. After overnight incubation, the mating plates were then replica plated onto SC medium selective for diploids and further incubated at 30 °C for 2–3 d. The mating response of *MAT***a** cells was also assessed by the level of pheromone-induced growth inhibition, using an agar diffusion (halo) bioassay (35), in which sterile filter disks spotted with 15 μL of a 1 mg/mL stock of α-factor mating pheromone were placed on a lawn of cells and incubated at 30 °C for 2–3 d. To measure the level of expression of a *FUS1$_{prom}$-lacZ* reporter gene, exponentially growing cells were incubated with and without 3–5 μM α-factor for 90 min. The amount of β-galactosidase produced then was measured using a colorimetric substrate as described elsewhere (36).

Fluorescence Microscopy, Image Acquisition, Processing, and Analysis. Transformants expressing GFP fusions were grown to midexponential phase, treated with α-factor (where necessary), and prepared for microscopic examination by either standard epifluorescence or deconvolution fluorescence microscopy, as indicated. For deconvolution microscopy, cells were viewed under a 100× objective using a Delta-Vision Spectris DV4 deconvolution microscope (Applied Precision). Images were collected and processed using API SoftWoRx imaging software and Photoshop (Adobe Systems). For standard epifluorescence microscopy, cells were concentrated and immediately thereafter, the cells were immobilized on an agarose pad and examined under an epifluorescence microscope (Olympus model BH-2), using a 100×

objective. GFP (green) fluorescence was assessed using a 470-nm (40-nm bandwidth) excitation filter and a 525-nm (50-nm bandwidth) emission filter (Endow GFP 47001; Chroma Technology), and mCherry (red) fluorescence was imaged using a 560-nm (40-nm bandwidth) excitation filter and a 630-nm (60-nm bandwidth) emission filter (31004 Texas Red; Chroma). Images were collected by using a charged-coupled device camera (Olympus) and then digitally processed and recorded with Magnafire SP imaging software (Optronics) and Adobe Photoshop.

Yeast Cell Lysis and Activated MAPK Analysis. Yeast cells were grown at the indicated temperature to midexponential phase ($A_{600\ nm}$ = 0.6–0.8), harvested by centrifugation, washed once with ice-cold PBS, and then snap frozen in liquid N_2. The frozen pellets were resuspended by vortex mixing in 150 μL of 1.85 M NaOH and 7.4% β-mercaptoethanol and incubated for 10 min on ice, and then ice-cold trichloroacetic acid (TCA) (25% final concentration) was added. After 10 min on ice, the precipitated protein was collected by centrifugation at maximum speed in a microfuge at 4 °C, washed twice with ice-cold acetone to remove residual TCA, and resuspended in an appropriate volume (32 μL per $A_{600\ nm}$) of 5% SDS in 0.1 M untitered Tris Base. For SDS/polyacrylamide gel electrophoresis (PAGE) of such samples, 8 μL (per $A_{600\ nm}$) of 5× concentrated SDS/PAGE sample buffer was added to each and, after boiling for 2 min and clarification by centrifugation in a microfuge, a portion (typically ~10 μL or ~0.25 $A_{600\ nm}$) of the resulting supernatant solution was resolved by SDS/PAGE on an 8% slab gel, transferred to a nitrocellulose membrane, and analyzed by immunoblotting. To detect activated Fus3, the membrane was incubated with rabbit polyclonal anti-phospho-p44/p42 antibody (Cell Signaling) and with goat polyclonal anti-Fus3 antibody (Santa Cruz Biotechnology) to assess total Fus3 and then washed, incubated with anti-rabbit and anti-goat infra-red fluorophore-conjugated secondary antibodies, visualized using an infrared imaging system (Odyssey; Li-Cor Biosciences), and quantified with the Odyssey Software v 2.1 (Li-Cor Biosciences).

ACKNOWLEDGMENTS. We thank Peter Pryciak (University of Massachusetts Medical Center) for the gift of plasmids pPP1872 and pPP1968, Bret Judson (Weill Institute Imaging Facility) for assistance with FRAP analysis, and all members of the Thorner Lab for advice and helpful discussion. This work was supported by National Institutes of Health Predoctoral Traineeships GM07232 and CA09041 (to L.S.G.), the Howard Hughes Medical Institute and by a research award from Cornell University (to C.J.S. and S.D.E.), Jane Coffin Childs Postdoctoral Research Fellowship 61-1295 (to M.A.M.), and National Institutes of Health R01 Research Grant GM21841 (to J.T.).

1. McLaughlin S, Wang J, Gambhir A, Murray D (2002) PIP($_2$) and proteins: Interactions, organization, and information flow. *Annu Rev Biophys Biomol Struct* 31:151–175.
2. Janmey PA, Lindberg U (2004) Cytoskeletal regulation: Rich in lipids. *Nat Rev Mol Cell Biol* 5:658–666.
3. Simonsen A, Wurmser AE, Emr SD, Stenmark H (2001) The role of phosphoinositides in membrane transport. *Curr Opin Cell Biol* 13:485–492.
4. Downes CP, Gray A, Lucocq JM (2005) Probing phosphoinositide functions in signaling and membrane trafficking. *Trends Cell Biol* 15:259–268.
5. Janetopoulos C, Devreotes P (2006) Phosphoinositide signaling plays a key role in cytokinesis. *J Cell Biol* 174:485–490.
6. Bagorda A, Mihaylov VA, Parent CA (2006) Chemotaxis: Moving forward and holding on to the past. *Thromb Haemost* 95:12–21.
7. Martin-Belmonte F, et al. (2007) PTEN-mediated apical segregation of phosphoinositides controls epithelial morphogenesis through Cdc42. *Cell* 128:383–397.
8. Heo WD, et al. (2006) PI(3,4,5)P_3 and PI(4,5)P_2 lipids target proteins with polybasic clusters to the plasma membrane. *Science* 314:1458–1461.
9. Ziel JW, Hagedorn EJ, Audhya A, Sherwood DR (2009) UNC-6 (netrin) orients the invasive membrane of the anchor cell in *C. elegans*. *Nat Cell Biol* 11:183–189.
10. Strahl T, Thorner J (2007) Synthesis and function of membrane phosphoinositides in budding yeast, *Saccharomyces cerevisiae*. *Biochim Biophys Acta* 1771:353–404.
11. Garrenton LS, Young SL, Thorner J (2006) Function of the MAPK scaffold protein, Ste5, requires a cryptic PH domain. *Genes Dev* 20:1946–1958.
12. Hurley JH, Meyer T (2001) Subcellular targeting by membrane lipids. *Curr Opin Cell Biol* 13:146–152.
13. Lemmon MA, Ferguson KM (2000) Signal-dependent membrane targeting by pleckstrin homology (PH) domains. *Biochem J* 350:1–18.
14. Inouye C, Dhillon N, Thorner J (1997) Ste5 RING-H2 domain: Role in Ste4-promoted oligomerization for yeast pheromone signaling. *Science* 278:103–106.
15. Stefan CJ, Audhya A, Emr SD (2002) The yeast synaptojanin-like proteins control the cellular distribution of phosphatidylinositol (4,5)-bisphosphate. *Mol Biol Cell* 13: 542–557.
16. Hilgemann DW (2007) Local PIP(2) signals: When, where, and how? *Pflugers Arch* 455:55–67.
17. Winters MJ, Lamson RE, Nakanishi H, Neiman AM, Pryciak PM (2005) A membrane binding domain in the ste5 scaffold synergizes with gbetagamma binding to control localization and signaling in pheromone response. *Mol Cell* 20:21–32.
18. Audhya A, Emr SD (2002) Stt4 PI 4-kinase localizes to the plasma membrane and functions in the Pkc1-mediated MAP kinase cascade. *Dev Cell* 2:593–605.
19. Strahl T, Hama H, DeWald DB, Thorner J (2005) Yeast phosphatidylinositol 4-kinase, Pik1, has essential roles at the Golgi and in the nucleus. *J Cell Biol* 171:967–979.
20. Orlando K, et al. (2008) Regulation of Gic2 localization and function by phosphatidylinositol 4,5-bisphosphate during the establishment of cell polarity in budding yeast. *J Biol Chem* 283: 14205–14212.
21. Qi M, Elion EA (2005) Formin-induced actin cables are required for polarized recruitment of the Ste5 scaffold and high level activation of MAPK Fus3. *J Cell Sci* 118:2837–2848.
22. Ayscough KR, et al. (1997) High rates of actin filament turnover in budding yeast and roles for actin in establishment and maintenance of cell polarity revealed using the actin inhibitor latrunculin-A. *J Cell Biol* 137:399–416.
23. Bardwell L (2005) A walk-through of the yeast mating pheromone response pathway. *Peptides* 26:339–350.
24. Slessareva JE, Routt SM, Temple B, Bankaitis VA, Dohlman HG (2006) Activation of the phosphatidylinositol 3-kinase Vps34 by a G protein alpha subunit at the endosome. *Cell* 126:191–203.
25. Flatauer LJ, Zadeh SF, Bardwell L (2005) Mitogen-activated protein kinases with distinct requirements for Ste5 scaffolding influence signaling specificity in *Saccharomyces cerevisiae*. *Mol Cell Biol* 25:1793–1803.
26. Sette C, Inouye CJ, Stroschein SL, Iaquinta PJ, Thorner J (2000) Mutational analysis suggests that activation of the yeast pheromone response mitogen-activated protein kinase pathway involves conformational changes in the Ste5 scaffold protein. *Mol Biol Cell* 11:4033–4049.
27. Good M, Tang G, Singleton J, Reményi A, Lim WA (2009) The Ste5 scaffold directs mating signaling by catalytically unlocking the Fus3 MAP kinase for activation. *Cell* 136:1085–1097.
28. Stolz LE, Huynh CV, Thorner J, York JD (1998) Identification and characterization of an essential family of inositol polyphosphate 5-phosphatases (*INP51*, *INP52* and *INP53* gene products) in the yeast *Saccharomyces cerevisiae*. *Genetics* 148:1715–1729.
29. Emoto K, Inadome H, Kanaho Y, Narumiya S, Umeda M (2005) Local change in phospholipid composition at the cleavage furrow is essential for completion of cytokinesis. *J Biol Chem* 280:37901–37907.
30. Field SJ, et al. (2005) PtdIns(4,5)P_2 functions at the cleavage furrow during cytokinesis. *Curr Biol* 15:1407–1412.
31. Ciejek E, Thorner J (1979) Recovery of *S. cerevisiae* a cells from G1 arrest by alpha factor pheromone requires endopeptidase action. *Cell* 18:623–635.
32. Sherman F, Fink GR, Hicks JB (1986) *Laboratory Course Manual for Methods in Yeast Genetics* (Cold Spring Harbor Lab Press, Cold Spring Harbor, NY).
33. Sambrook J, Fritsch EF, Maniatis T (1989) *Molecular Cloning: A Laboratory Manual* (Cold Spring Harbor Lab Press, Cold Spring Harbor, NY), 2nd Ed.
34. Sprague GF, Jr (1991) Assay of yeast mating reaction. *Methods Enzymol* 194:77–93.
35. Reneke JE, Blumer KJ, Courchesne WE, Thorner J (1988) The carboxy-terminal segment of the yeast alpha-factor receptor is a regulatory domain. *Cell* 55:221–234.
36. Stern M, Jensen R, Herskowitz I (1984) Five *SWI* genes are required for expression of the *HO* gene in yeast. *J Mol Biol* 178:853–868.